Cellular and Molecular Biology
E-ISSN : 1165-158X / P-ISSN : 0145-5680
www.cellmolbiol.org

Analysis of Macrophage Chemotactic Activity and TLR9 Signaling Pathway in the Mouse Model of Viral Acute Lung Injury

Yingpu Li[1#], Ju Xiong[1#], Wanhan Ye[2*]

[1] Department of Emergency, the First People's Hospital of Jiangxia District, Wuhan 430299, Hubei Province, China
[2] Department of Emergency, Yunjingshan Hospital, Jiangxia District, Wuhan 430207, Hubei Province, China

[#]These authors contributed equally to this work as co-first author

ARTICLE INFO

Original paper

Article history:
Received: September 11, 2022
Accepted: November 17, 2022
Published: November 30, 2022

Keywords:

Viral acute lung injury, Macrophages, chemokines, chemotactic activity, inflammatory cytokines, TLR9

ABSTRACT

This study focused on the chemotactic activity of macrophages and the role of the TLR9 signaling pathway in the pathogenesis of viral Acute Lung Injury (ALI). For this purpose, a total of 40 male SPF mice were used, aged 5-8 weeks. They were randomly divided into an experimental group and a control group. The experimental group was further divided into S1 and S2, and the control group was further divided into D1 and D2, with 10 in each. The different groups were detected for the expression of inflammatory cytokines and chemokines and the expression of alveolar macrophages. Results showed that as for the weight, survival status, arterial blood gas analysis, lung index and wet-to-dry value of lung tissue, and lung histopathological analysis results, the S2 group showed more obvious changes versus the D2 group, and the difference was statistically significant (P<0.05). S2 had higher levels of the inflammatory factors TNF-α, IL-1β, IL-6 and the chemokine CCL3 in the BALF supernatant versus the D2 Group, and the difference is statistically significant (P<0.05). S2 had higher expression levels of chemokines CCR5, TLR9, and JMJD1A mRNA versus the D2 group, and the difference was statistically significant (P<0.05). In conclusion, the establishment of a mouse ALI model induced by poly l:C was successful; AM has a certain chemotactic activity on CCL3; polyI:C can promote the expression activity and chemotactic activity of macrophages CCR5 through signal pathways, such as TLR9.

Doi: http://dx.doi.org/10.14715/cmb/2022.68.11.12

Introduction

Acute lung injury (ALI) refers to acute hypoxic respiratory insufficiency or breathing failure arising from diffuse pulmonary edema due to injury to microvascular endothelial cells and alveolar epithelial cells. It will develop into Acute respiratory distress syndrome (ARDS) at a severe stage, so the pathological process of ALI and ARDS is the same (1-3). As per statistics, the mortality rate of ARDS in China reaches 44.8% (4). The main pathogenic factors of ALI are infection, external trauma, shock, and inhalation. Children are predominantly affected by infections, which are divided into viral and bacterial infections (5). The pathogenesis of ALI and ARDS in children is complicated, and the fatality rate is very high. Therefore, they have become a focus in the field of basic and clinical critical care medicine (6).

Macrophages (mø), a kind of immune cells, derived from monocytes, mainly engulf pathogens and activate immune cells (7). The macrophages in the alveolar tissue, namely, alveolar macrophage (AM), can be regarded as the first line of immune defense of the lung organs. When the lung tissue is stimulated, it will produce a variety of inflammatory mediators, to promote or inhibit the inflammatory reaction process through various mechanisms (8). Although the dual effects of AM seem to be contradictory, it is actually composed of two kinds of cells: colonized alveolar macrophages and recruited alveolar macrophages. AMs are instrumental in the development of ALI disease (9,10). At the early stage of ALI, activated monocytes enter the lung before the clinical symptoms appear (11). After infection, neutralizing the up-regulated chemokines in the lung tissue can inhibit the accumulation of AM and injury to the lung (12). Moreover, infectious pathogens can stimulate the expression of chemokine receptors, so that their expression is correspondingly increased (13). Bacterial-related endotoxins are a recognized mononuclear/macrophage activator in the development of ALI. Studies have shown that virus infection has a similar effect on the recruitment of alveolar macrophages (14). DNA receptors and macrophages have similar characteristics. They are in the cytoplasm and equivalent to a recognition receptor, which can quickly identify pathogens and activate innate and adaptive immune responses. It has been discovered that the DNA sensor can be used as a genetic vaccine adjuvant (15).

Toll-like receptors (TLRs) are a part of the innate immune system, and their main function is to recognize and stimulate the immune system to kill pathogens (16). Studies have revealed that, TLR can accelerate the development of ALI, and that TLR can recognize pathogen-associated molecular patterns (PAMPs) and unmethylation DNA (Cp G DNA), or endogenous unmethylated DNA. As a result, the signal pathway mediated by TLR can be activated (17). TLR9 attracts more attention among TLRs. It can cause lung injury through a series of reactions, such

* Corresponding author. Email: linyi4516108326@163.com

as activation, phosphorylation, and release of inflammatory mediators (18).

In order to study the chemotactic activity of macrophages and the mechanism of the TLR9 signaling pathway in the development of ALI, in the study, viral ALI was analyzed, expected to provide a basis for clinical targeted treatment.

Materials and Methods

Basic information

Research subjects

In this study, 40 male SPF mice were used, aged 5 to 8 weeks. They were raised in an environment free of special pathogens, and the temperature was controlled between 20~24°C, and the humidity was controlled between 40% and 60%, with a 12-hour light/dark circle. They had free access to food and water for 24 hours. The experiment has been approved by the Chinese Medical Ethics Committee.

The grouping

They were randomly divided into an experimental group and a control group, and the experimental group was further divided into S1 and S2, and the control group was further divided into D1 and D2, with 10 in each group. They were raised in an environment free of special pathogens, and the temperature was controlled between 20~24°C, and the humidity was controlled between 40% and 60%, with a 12-hour light/dark circle. They had free access to food and water for 24 hours.

The viral ALI model

In the study, polyinosinic polycytidylic acid (Poly I: C) was used, and the specific process was shown in Figure 1.

After the model was established, its feasibility was analyzed. The evaluation content included regular weighing, observation and recording of survival status, arterial blood gas analysis, the lung index, the wet-to-dry ratio of lung tissue, and the histopathological analysis of the model mice.

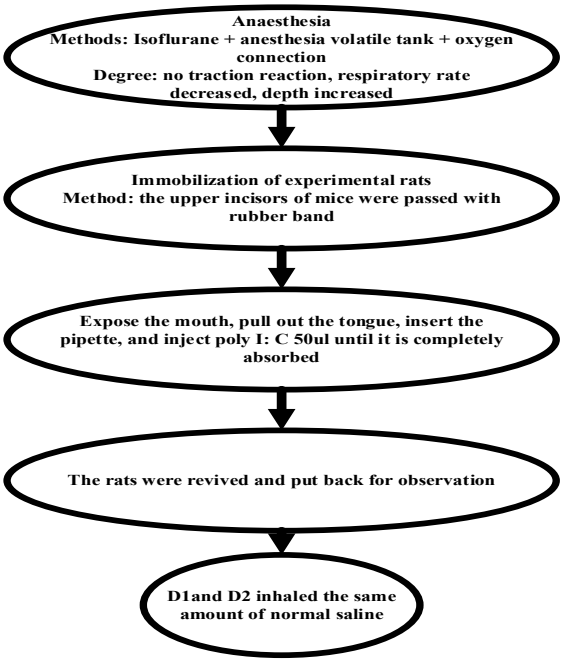

Figure 1. The process of establishing a viral ALI model.

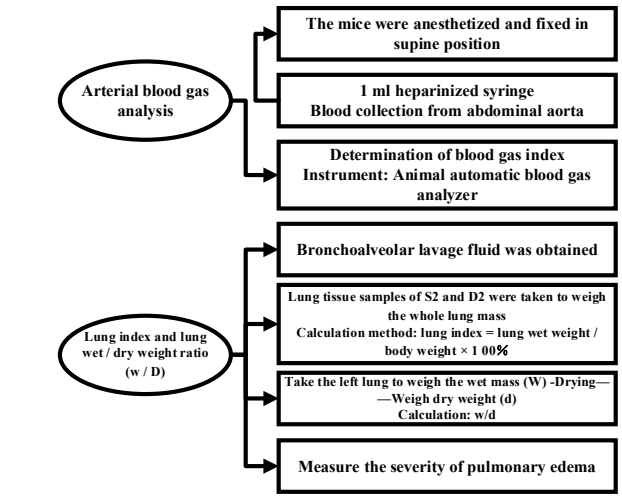

Figure 2. The arterial blood gas analysis, the lung index, and the wet-to-dry ratio of lung tissue.

The specific operation was as follows. The survival status of S1 and D1 was observed for 15 consecutive days. They were weighed regularly, and the probability of death was calculated. On the sixth day after the model was established, the mice in S2 and D2 were weighed, followed by the arterial blood gas analysis and the calculation of the lung index and the wet-to-dry ratio of lung tissue, as shown in Figure 2. Then, the right lung tissue was taken out for pathological analysis and fixed with 10% neutral formaldehyde for 24 hours, and then the following operations were as shown in Figure 3. After the pathological tissue sections were processed, they were visualized under an optical microscope, and the Smith scoring method (19) was used for semi-quantitative analysis, factoring into pulmonary edema, atelectasis and pulmonary hyaline membrane formation, alveolar and pulmonary interstitial inflammation, and hemorrhage. The specific scoring criteria were shown in Table 1. The average value of 10 results under a high-power microscope was taken as the lung tissue pathological damage score.

Research methods

(i) 2.5 mL bronchoalveolar lavage fluid (BALF) was collected from each mouse. Then, BALF was centrifuged to separate the macrophages and culture them.

(ii) the enzyme-linked immunosorbent assay (ELISA) was used to detect macrophage inflammatory factors, such as TNF-α, IL-1β, IL-6, and chemokine CCL3 in BALF supernatant;

(iii) the real-time quantitative polymerase chain reaction (PCR) method was used to detect the expression levels of CC chemokine receptor 5 (CCR5), TLR9, and JMJD1AmRNA in mouse alveolar macrophages.

(iv) plasma DNA was extracted from lung tissue, and fluorescence quantitative PCR was used to determine the DNA level. The plasma DNA concentration was calculated as follows.

$$c=Q\times VDNA/VPCR\times 1/VEXT \quad (1)$$

Where the c-the concentration of mtDNA in plasma; Q-the number of copies of mtDNA in the sample detected by fluorescence quantitative PCR; VDNA-the total volume of DNA extracted from each plasma sample.

Statistics

The SPSS22.0 was used to process the data, and the

Table 1. The scoring criteria of the 0~4 points semi-quantitative analysis.

Point	0	1	2	3	4
Lesion area	No injury	<25%	25%~50%	50%~75%	Full view

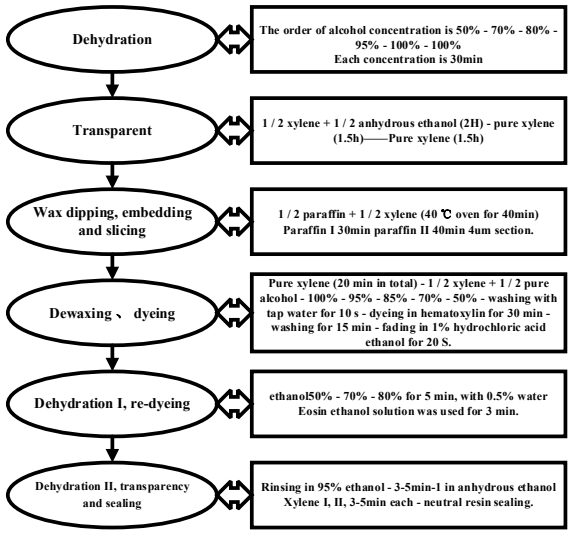

Figure 3. Pathological tissue section processing of right lung tissue of the model mouse.

measurement data in accordance with the normal distribution were expressed as mean ± standard deviation ($\bar{X} \pm s$), calculated to two decimal places. The in-group comparison was performed by paired t-test, and the comparison between the two groups was performed by independent t-test. Quantitative data conforming to skewed distribution were represented by median (range), and the Wilcoxon rank sum test was used for comparison between the two groups. Count data were expressed as a percentage (%), calculated to one decimal place, and the comparison between the two groups was used χ^2 test. The P was calculated to 3 decimal places, and $P<0.05$ was the threshold for significance.

Results

The survival status and weight of mice in S1 and D1

As for the survival status of the mice in the S1 and S2 treated with poly:C, it was found that they gradually lost weight, and have symptoms such as malaise, decreased activity, eating less, and increased breathing. There even appeared deaths on the 6th day. By the 15th day, there were 9 dead mice. Anatomy results of the lung tissue showed that the lung of the dead mice appeared edema, congestion, hemorrhage and there was bloody foamy liquid from the bronchus. Regular weight detection results showed that the weight of mice in S1 and S2 of the experimental group showed a downward trend, while the mice in the D1 group of the control group had no abnormalities, and the difference was statistically significant ($P<0.05$), as shown in Figure 4.

Blood gas analysis and W/D ratio in S2 and D2

On the sixth day after the model was established, the arterial blood gas analysis was performed on mice in S2 and D2. The results found that there was no notable difference in PH of the arterial blood of the two groups, and the difference was not statistically significant ($P>0.05$), while the S2 group showed lower PaO_2 and SaO_2 and higher PCO_2 versus the D2 group, and the difference was statistically significant ($P<0.05$), as shown in Figure 5. As for the lung index and W/D value of the lung tissue, the average lung indexes of the mice in the S2 group and D2 group were (0.65±0.03) and (2.01±0.08), respectively, and the W/D values were (6.01±1.61) and (3.12±2.15). The average lung index of the S2 group was higher than that of the D2 group, and the average W/D value was lower than that of the D2 group, and the difference was statistically significant ($P<0.05$), as shown in Figure 6. Taken together, the establishment of the mouse ALI model induced by poly I:C was successful.

Pathological analysis results in S2 and D2

The lung tissue slices of the two groups of mice were visualized through an optical microscope, as shown in Figure 7. It was noted that the lung tissue of the S2 group showed obvious alveolar lesions, such as alveolar wall edema and thickening, space shrinkage, and loose mesenchyme and even bleeding, and a large number of cells

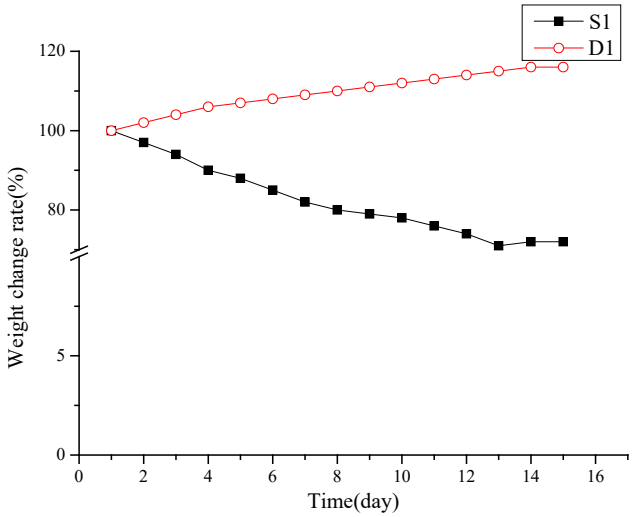

Figure 4. The weight change of mice in the S1 and the D1.

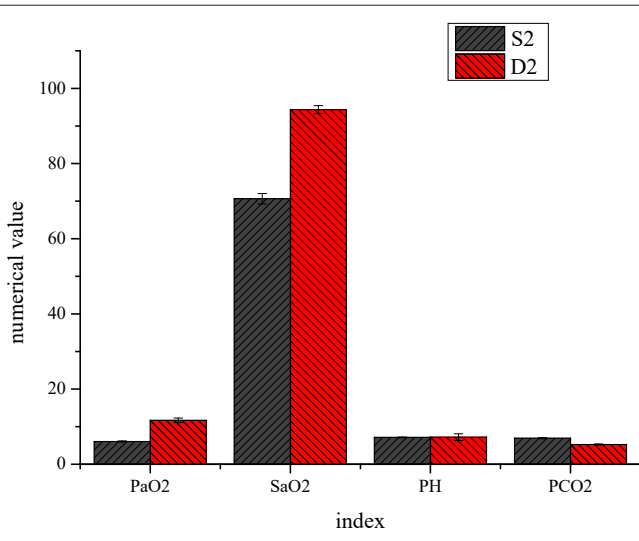

Figure 5. The results of arterial blood gas analysis between the S2 group and the D2 group.

appeared; but the lung tissue of the mice in the D2 group had no obvious lesions. As per the 0-4 points semi-quantitative analysis standard, the two groups were scored for pathological damage of lung tissue. The score of mice in group S2 was (6.01±0.18), and the score of mice in group D2 was (1.39±0.21). It was found that the pathological damage of mice in the S2 group was higher than that in the D2 group, and the difference was statistically significant (P<0.05), as shown in Figure 8, which further proved the success of the model established.

Expression of chemokine and cytokine in BALF supernatant of S2 and D2

During the study, the mice in S2 and the D2 were compared for the expression of inflammatory factors TNF-α, IL-1β, IL-6 and chemokine CCL3 in the BALF supernatant, as shown in Figure 9. It was noted that the expression activity of the above inflammatory factors and chemokines was significantly enhanced in mice in the S2 group versus the D2 group, which confirmed that, AM has a certain chemotactic effect on CCL3, and the increased expression activity of inflammatory factors increased further proved the success of the model established.

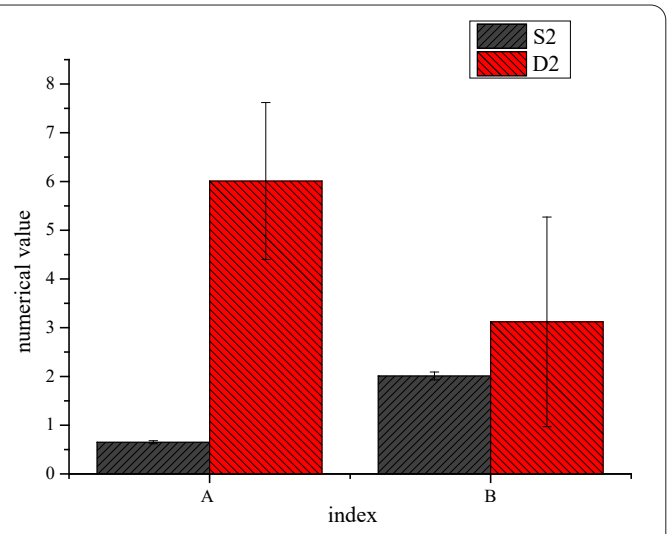

Figure 6. The lung index and W/D value between the S2 group and D2 group (A: lung index B: W/D value).

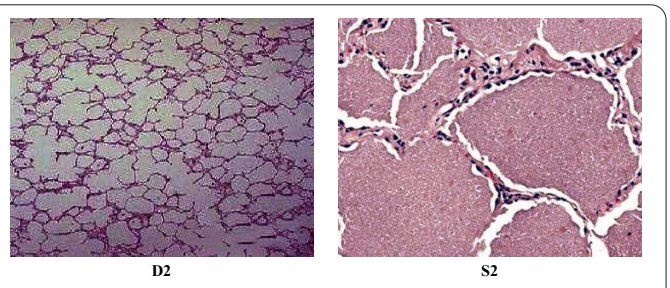

Figure 7. Histopathological analysis results in S2 and D2.

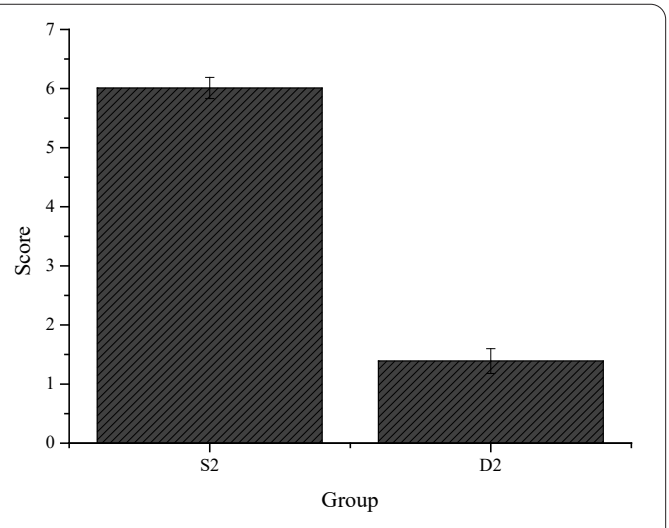

Figure 8. Lung tissue pathological damage scores in S2 and D2.

Expression of chemokine in S2 and D2

The mice in S2 and D2 were compared for the expression levels of chemokines CCR5, TLR9, JMJD1A mRNA, etc., as shown in Figure 10. It was noted that the expression activity of the S2 group was significantly higher than that of the D2 group, and the difference was statistically significant (P<0.05). It proved that viral ALI changed the activities of CCR5, TLR9, and JMJD1A in AM. It also showed that polyI:C can promote the expression and chemotactic activity of macrophages CCR5 through the TLR9 signaling pathway.

Plasma DNA levels in S2 and D2

The S2 and D2 were compared for the DNA content in the lung tissue, as shown in Figure 11. Obviously, the DNA concentration of the S2 group was higher than that

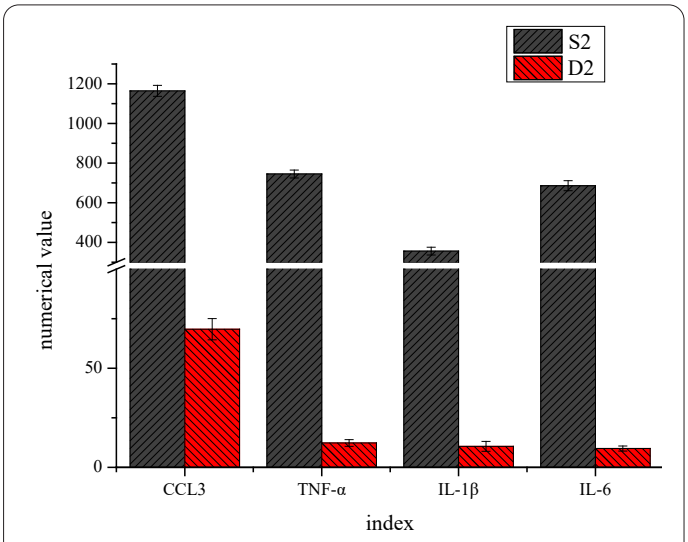

Figure 9. Expression of chemokines and inflammatory factors in the BALF supernatant of S2 and D2.

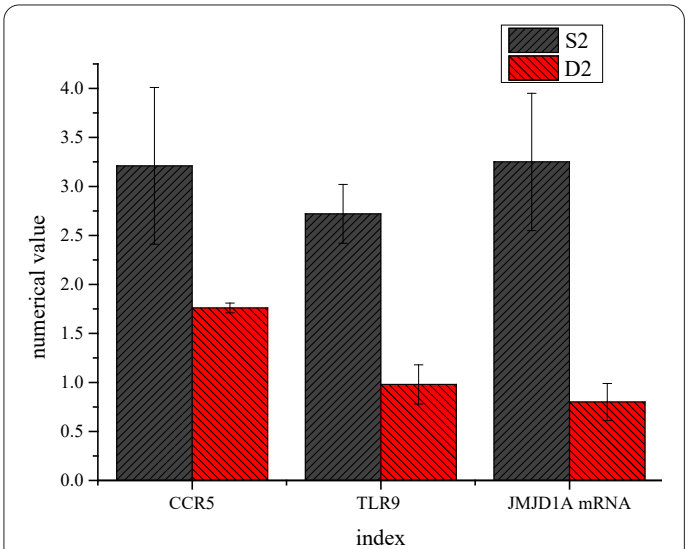

Figure 10. Expression of chemokine expression in S2 and D2.

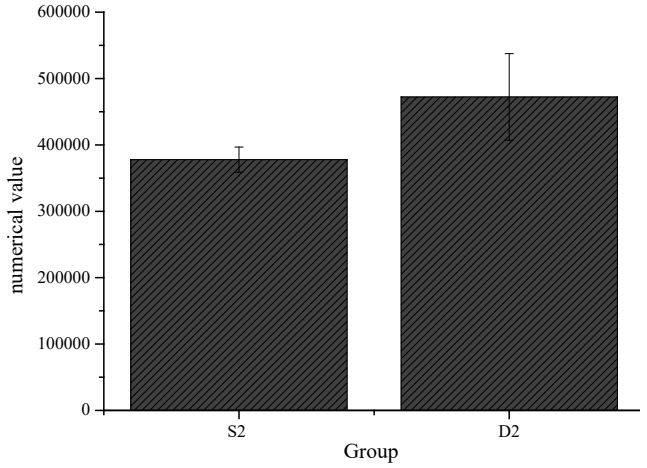

Figure 11. Plasma DNA levels in lung tissue in S2 and D2.

of the D2 group and the difference was statistically significant ($P<0.05$).

Discussion

In this study, a mouse model of viral ALI was established, and the mice inhaled polyI through the mouth. Groups were compared in terms of the expression activity of chemokine CCL3 and inflammatory factors TNF-α, IL-1β, and IL-6 in the BALF supernatant, and macrophages in the BALF were separated and cultured, to study the mechanism of their chemotactic activity in viral ALI. Despite learning from other experts (20), we evaluated the degree of lung injury in each group of mice through regular weighing, observation and recording of survival status, arterial blood gas analysis, the lung index and W/D value of lung tissue, and the pathological damage score under the lung histopathological analysis of the established model mice, thus confirming that the viral ALI mouse model induced by poly I: C was successfully established. At present, there are many induction methods to establish ALI animal models, such as the use of lipopolysaccharide (LPS), influenza virus, bleomycin, hypoxia, and ventilator (21-22). Studies have suggested that LPS can cause acute diffuse damage to alveolar tissue, activate inflammatory factors, and release a series of inflammatory mediators (23), further damaging the lung tissue. It is consistent with the results of the study. In this study, it was also found that the expression activity of the chemokine CCL3 of BALF in the viral ALI mouse model has been increased. Previously, research experts used LPS for induction to establish an ALI model, and found that the expression activity of CCL3 in lung tissue has also been increased, which aggravated inflammatory damage to the lung tissue, and it was inferred that the recruited macrophages and neutrophils of the lobular nucleus into the lung tissue may be the main factors leading to this reaction (24). It was also concluded in the study that, TLR9 and other signaling pathways enhanced the expression activity and chemotactic activity of macrophages CCR5. Previously, experts have conducted related studies on whether TLR9 signaling pathways can mediate the inflammatory response. During the research, they inhibited TLR9 and found that the phosphorylation level of c-Jun N-terminal kinase (JNK) and damage to the lung was reduced to a certain extent (25), which was in line with the research results of the study, and it also provided a new research direction to control ALI disease. Moreover, the main reason for using mice to establish a model in this study is that TLR9 has certain similarities to different species. TLR9 derived from mice and TLR9 derived from Homo sapiens are both encoded by 1032 amino acids, and approximately 77% of the amino acid codes are consistent (26), so the accuracy of the experimental results was high for other animal models. Studies have found that TLR9 is not only related to the development of ALI, but also associated with autoimmune diseases, malignant tumors, and other diseases. For autoimmune diseases, generally, the DNA structure of mammals is histone-encapsulated methylated DNA. In this state, the methylation motif cannot activate TLR9. Only under certain pathological conditions, the imbalance of methylation/demethylation may increase the level of self-unmethylated DNA and activate the TLR9 signaling pathway. Uncontrolled inflammation leads to the occurrence of autoimmune diseases, and the high expression of TLR9 also occurs in idiopathic pulmonary fibrosis (27). For tumor diseases, the expression of TLR9 is higher in lung cancer tissue versus in normal lung tissue (28-29). For ALI, TLR9 can be activated by mitochondrial DNA and cause secondary lung injury (30).

It has been proposed that some DNA receptors can be used as adjuvants for genetic vaccines, that DNA plasmids and their metabolites can directly interact with DNA receptors as antigens, and that DNA entering the cytoplasm of cells (considered by the body as a danger signal of pathogen infection) can be recognized and bind to DNA receptors to rapidly activate the innate immune response so that a large amount of I type interferon (IFN) is produced in fibroblasts, macrophages and dendritic cells to enhance the immune effect of DNA vaccine (31). However, whether this method can be applied to the clinical treatment of viral ALI remains to be studied.

Conclusion

In this study, polyI:C was used to induce the viral ALI mouse model, and then the AM in the SALF of the mice in each group was extracted to detect its chemotaxis factors and expression activity of the TLR9 signaling pathway. The results of the study found that, polyl:C can mediate macrophage activation and recruitment to participate in viral ALI by promoting the expression of macrophages CCR3 and its chemotactic activity on CCL3. This reaction was mediated through the TLR9 signaling pathway. PolyI:C inhibited the level of H3K9me2 in the promoter region of CCR5 by promoting the expression of histone demethylase JMJD1A.

However, this study only explores the effects of virus-related products on the chemotactic activity of macrophages, chemokines, and related signal pathways. In the follow-up, a more in-depth research is needed on the etiology and pathogenesis of ALI, so as to provide a theoretical basis for the clinical treatment of ALI.

References

1. Kellner M, Noonepalle S, Lu Q, Srivastava A, Zemskov E, Black SM. ROS Signaling in the Pathogenesis of Acute Lung Injury (ALI) and Acute Respiratory Distress Syndrome (ARDS). Adv Exp Med Biol 2017; 967: 105-137. doi: 10.1007/978-3-319-63245-2_8. PMID: 29047084; PMCID: PMC7120947.
2. Xu J, Yang J, Chen J, Luo Q, Zhang Q, Zhang H. Vitamin D alleviates lipopolysaccharide-induced acute lung injury via regulation

of the renin-angiotensin system. Mol Med Rep 2017 Nov; 16(5): 7432-7438. doi: 10.3892/mmr.2017.7546. Epub 2017 Sep 20. PMID: 28944831; PMCID: PMC5865875.

3. Rajasekaran S, Pattarayan D, Rajaguru P, Sudhakar Gandhi PS, Thimmulappa RK. MicroRNA Regulation of Acute Lung Injury and Acute Respiratory Distress Syndrome. J Cell Physiol 2016 Oct; 231(10): 2097-106. doi: 10.1002/jcp.25316. Epub 2016 Feb 4. PMID: 26790856.
4. Komiya K, Akaba T, Kozaki Y, Kadota JI, Rubin BK. A systematic review of diagnostic methods to differentiate acute lung injury/acute respiratory distress syndrome from cardiogenic pulmonary edema. Crit Care 2017 Aug 25; 21(1): 228. doi: 10.1186/s13054-017-1809-8. PMID: 28841896; PMCID: PMC6389074.
5. Khatri M, Richardson LA, Meulia T. Mesenchymal stem cell-derived extracellular vesicles ttenuate influenza virus-induced acute lung injury in a pig model. Stem Cell Res Ther 2018 Jan 29; 9(1): 17. doi: 10.1186/s13287-018-0774-8. PMID: 29378639; PMCID: PMC5789598.
6. El Basset Abo El Ezz AA, Abd El Hafez MA, El Amrousy DM, El Momen Suliman GA. The predictive value of Von Willebrand factor antigen plasma levels in children with acute lung injury. Pediatr Pulmonol 2017 Jan; 52(1): 91-97. doi: 10.1002/ppul.23518. Epub 2016 Jun 30. PMID: 27362747.
7. Oishi Y, Manabe I. Macrophages in inflammation, repair and regeneration. Int Immunol 2018 Oct 29; 30(11): 511-528. doi: 10.1093/intimm/dxy054. PMID: 30165385.
8. Joshi N, Walter JM, Misharin AV. Alveolar Macrophages. Cell Immunol 2018 Aug; 330: 86-90. doi: 10.1016/j.cellimm.2018.01.005. Epub 2018 Jan 20. PMID: 29370889.
9. Soni S, Wilson MR, O'Dea KP, Yoshida M, Katbeh U, Woods SJ, Takata M. Alveolar macrophage-derived microvesicles mediate acute lung injury. Thorax 2016 Nov; 71(11): 1020-1029. doi: 10.1136/thoraxjnl-2015-208032. Epub 2016 Jun 10. PMID: 27287089; PMCID: PMC5099194.
10. Fan EKY, Fan J. Regulation of alveolar macrophage death in acute lung inflammation. Respir Res 2018 Mar 27; 19(1):50. doi: 10.1186/s12931-018-0756-5. PMID: 29587748; PMCID: PMC5872399.
11. Hou L, Yang Z, Wang Z, Zhang X, Zhao Y, Yang H, Zheng B, Tian W, Wang S, He Z, Wang X. NLRP3/ASC-mediated alveolar macrophage pyroptosis enhances HMGB1 secretion in acute lung injury induced by cardiopulmonary bypass. Lab Invest 2018 Aug; 98(8): 1052-1064. doi: 10.1038/s41374-018-0073-0. Epub 2018 Jun 8. PMID: 29884910.
12. Huang X, Xiu H, Zhang S, Zhang G. The Role of Macrophages in the Pathogenesis of ALI/ARDS. Mediators Inflamm 2018 May 13; 2018: 1264913. doi: 10.1155/2018/1264913. PMID: 29950923; PMCID: PMC5989173.
13. Zhang P, Fan Y, Li Q, Chen J, Zhou W, Luo Y, Zhang J, Su L, Xue X, Zhou X, Feng Y. Macrophage activating factor: A potential biomarker of periodontal health status. Arch Oral Biol 2016 Oct; 70: 94-99. doi: 10.1016/j.archoralbio.2016.06.010. Epub 2016 Jun 9. PMID: 27341461.
14. Che KF, Kaarteenaho R, Lappi-Blanco E, Levänen B, Sun J, Wheelock Å, Palmberg L, Sköld CM, Lindén A. Interleukin-26 Production in Human Primary Bronchial Epithelial Cells in Response to Viral Stimulation: Modulation by Th17 cytokines. Mol Med 2017 Oct; 23: 247-257. doi: 10.2119/molmed.2016.00064. Epub 2017 Aug 29. PMID: 28853490; PMCID: PMC5653736.
15. Dunphy G, Flannery SM, Almine JF, Connolly DJ, Paulus C, Jønsson KL, Jakobsen MR, Nevels MM, Bowie AG, Unterholzner L. Non-canonical Activation of the DNA Sensing Adaptor STING by ATM and IFI16 Mediates NF-κB Signaling after Nuclear DNA Damage. Mol Cell 2018 Sep 6; 71(5): 745-760.e5. doi: 10.1016/j.molcel.2018.07.034. PMID: 30193098; PMCID: PMC6127031.
16. Pelka K, Bertheloot D, Reimer E, Phulphagar K, Schmidt SV, Christ A, Stahl R, Watson N, Miyake K, Hacohen N, Haas A, Brinkmann MM, Marshak-Rothstein A, Meissner F, Latz E. The Chaperone UNC93B1 Regulates Toll-like Receptor Stability Independently of Endosomal TLR Transport. Immunity 2018 May 15; 48(5): 911-922.e7. doi: 10.1016/j.immuni.2018.04.011. PMID: 29768176; PMCID: PMC6482051.
17. Herrtwich L, Nanda I, Evangelou K, Nikolova T, Horn V, Sagar, Erny D, Stefanowski J, Rogell L, Klein C, Gharun K, Follo M, Seidl M, Kremer B, Münke N, Senges J, Fliegauf M, Aschman T, Pfeifer D, Sarrazin S, Sieweke MH, Wagner D, Dierks C, Haaf T, Ness T, Zaiss MM, Voll RE, Deshmukh SD, Prinz M, Goldmann T, Hölscher C, Hauser AE, Lopez-Contreras AJ, Grün D, Gorgoulis V, Diefenbach A, Henneke P, Triantafyllopoulou A. DNA Damage Signaling Instructs Polyploid Macrophage Fate in Granulomas. Cell 2016 Nov 17; 167(5): 1264-1280.e18. doi: 10.1016/j.cell.2016.09.054. Epub 2016 Oct 27. Erratum in: Cell. 2018 Aug 23;174(5):1325-1326. PMID: 28084216.
18. Yang C, Song Y, Wang H. Suppression of RAGE and TLR9 by Ketamine Contributes to Attenuation of Lipopolysaccharide-Induced Acute Lung Injury. J Invest Surg 2017 Jun; 30(3): 177-186. doi: 10.1080/08941939.2016.1232448. Epub 2016 Oct 7. PMID: 27715346.
19. Soto GJ, Kor DJ, Park PK, Hou PC, Kaufman DA, Kim M, Yadav H, Teman N, Hsu MC, Shvilkina T, Grewal Y, De Aguirre M, Gunda S, Gajic O, Gong MN. Lung Injury Prediction Score in Hospitalized Patients at Risk of Acute Respiratory Distress Syndrome. Crit Care Med 2016 Dec; 44(12): 2182-2191. doi: 10.1097/CCM.0000000000002001. PMID: 27513358; PMCID: PMC5431079.
20. Song N, Li P, Jiang Y, Sun H, Cui J, Zhao G, Li D, Guo Y, Chen Y, Gao J, Sun S, Zhou Y. C5a receptor1 inhibition alleviates influenza virus-induced acute lung injury. Int Immunopharmacol 2018 Jun; 59: 12-20. doi: 10.1016/j.intimp.2018.03.029. Epub 2018 Apr 2. PMID: 29621732.
21. Wang Y, Song Z, Bi J, Liu J, Tong L, Song Y, Bai C, Zhu X. A20 protein regulates lipopolysaccharide-induced acute lung injury by downregulation of NF-κB and macrophage polarization in rats. Mol Med Rep 2017 Oct; 16(4): 4964-4972. doi: 10.3892/mmr.2017.7184. Epub 2017 Aug 7. PMID: 28791391.
22. Coates BM, Staricha KL, Koch CM, Cheng Y, Shumaker DK, Budinger GRS, Perlman H, Misharin AV, Ridge KM. Inflammatory Monocytes Drive Influenza A Virus-Mediated Lung Injury in Juvenile Mice. J Immunol 2018 Apr 1; 200(7): 2391-2404. doi: 10.4049/jimmunol.1701543. Epub 2018 Feb 14. PMID: 29445006; PMCID: PMC5860989.
23. Xu J, Yang J, Chen J, Luo Q, Zhang Q, Zhang H. Vitamin D alleviates lipopolysaccharide-induced acute lung injury via regulation of the renin-angiotensin system. Mol Med Rep 2017 Nov; 16(5): 7432-7438. doi: 10.3892/mmr.2017.7546. Epub 2017 Sep 20. PMID: 28944831; PMCID: PMC5865875.
24. Lei J, Wei Y, Song P, Li Y, Zhang T, Feng Q, Xu G. Cordycepin inhibits LPS-induced acute lung injury by inhibiting inflammation and oxidative stress. Eur J Pharmacol 2018 Jan 5; 818: 110-114. doi: 10.1016/j.ejphar.2017.10.029. Epub 2017 Oct 18. PMID: 29054740.
25. Shaker ME, Trawick BN, Mehal WZ. The novel TLR9 antagonist COV08-0064 protects from ischemia/reperfusion injury in non-steatotic and steatotic mice livers. Biochem Pharmacol 2016 Jul 15; 112: 90-101. doi: 10.1016/j.bcp.2016.05.003. Epub 2016 May 6. PMID: 27157410.
26. Hotz MJ, Qing D, Shashaty MGS, Zhang P, Faust H, Sondheimer N, Rivella S, Worthen GS, Mangalmurti NS. Red Blood

Cells Homeostatically Bind Mitochondrial DNA through TLR9 to Maintain Quiescence and to Prevent Lung Injury. Am J Respir Crit Care Med 2018 Feb 15; 197(4): 470-480. doi: 10.1164/rccm.201706-1161OC. PMID: 29053005; PMCID: PMC5821907.

27. Farrokhi S, Abbasirad N, Movahed A, Khazaei HA, Pishjoo M, Rezaei N. TLR9-based immunotherapy for the treatment of allergic diseases. Immunotherapy 2017 Mar; 9(4): 339-346. doi: 10.2217/imt-2016-0104. PMID: 28303762.
28. Wang D, Jiang W, Zhu F, Mao X, Agrawal S. Modulation of the tumor microenvironment by intratumoral administration of IMO-2125, a novel TLR9 agonist, for cancer immunotherapy. Int J Oncol 2018 Sep; 53(3): 1193-1203. doi: 10.3892/ijo.2018.4456. Epub 2018 Jun 27. PMID: 29956749.
29. Martínez-Campos C, Burguete-García AI, Madrid-Marina V. Role of TLR9 in Oncogenic Virus-Produced Cancer. Viral Immunol 2017 Mar; 30(2): 98-105. doi: 10.1089/vim.2016.0103. Epub 2017 Feb 2. PMID: 28151089.
30. Shen H, Wu N, Wang Y, Zhang L, Hu X, Chen Z, Zhao M. Toll-like receptor 9 mediates paraquat-induced acute lung injury: an in vitro and in vivo study. Life Sci 2017 Jun 1; 178: 109-118. doi: 10.1016/j.lfs.2017.03.021. Epub 2017 Mar 29. PMID: 28363843.
31. Cao DJ, Schiattarella GG, Villalobos E, Jiang N, May HI, Li T, Chen ZJ, Gillette TG, Hill JA. Cytosolic DNA Sensing Promotes Macrophage Transformation and Governs Myocardial Ischemic Injury. Circulation 2018 Jun 12; 137(24): 2613-2634. doi: 10.1161/CIRCULATIONAHA.117.031046. Epub 2018 Feb 1. PMID: 29437120; PMCID: PMC5997506.